Entanglements in Inhomogeneous Polymeric Phases

Venkat Ganesan* and Victor Pryamitsyn

Department of Chemical Engineering, University of Texas at Austin, Austin, Texas 78712

Received June 13, 2002

ABSTRACT: We examine the concept of entanglements and the associated entanglement lengths in polymer interfaces. Explicitly, we consider the influence of the compositional inhomogeneity and the manner in which it influences the entanglement lengths. We address this issue by adapting the packing model of entanglements proposed by Kavassalis and Noolandi. The effects of the compositional inhomogeneity are incorporated through a combination of Monte Carlo simulations and self-consistent-field theory computations. Our results mainly focus on the inhomogeneous variations of entanglements in the interfacial region of polymer blends. In this context, we elaborate upon the connections between our results and the experimentally measurable macroscopic properties like the slip, rheology, and the toughness of polymer−polymer interfaces.

I. Introduction

High molecular weight polymer melts and concentrated solutions of polymers are characterized by the presence of a variety of topological interactions between the chains. Such interactions include physical crossings, knottings, and loopings and, in some cases, can even result from local energetic interactions like hydrogen bonding. Such features prove extremely complex to model accurately, and consequently it is a common approach to replace such interactions generically by fictitious constraining junctions termed as "entanglements" acting on different points of a chain.[1] Indeed, this physical picture formed the basis of the immensely successful Doi and Edwards (DE) reptation model for the dynamics of polymer melts.[2,3] In their model, the topological constraints were assumed to restrict the motion of long chains to essentially one dimension, viz., along a tube of confining entanglements. With this underlying basis, the DE theory replaced the conformation of the real chain by a connected sequence of "entanglement blobs" of size N_e, termed as the entanglement length of the polymer (in this article, we use the terms "entanglement length" and "entanglement molecular weight" in an interchangeable manner) and was envisioned to characterize the radius of the confinement tube. These blobs were then assumed to move in the tube by a diffusional mechanism which involved the creation and destruction of material at the ends of the tube. This approach allowed Doi and Edwards to make predictions for the self-diffusivity as well as the linear and nonlinear rheological properties of entangled polymer melts. Several of these predictions have been subsequently validated through experiments and have lent support to the underlying framework of "junction" model of topological constraints.[4]

Several recent experiments have highlighted a pivotal role for the value of the entanglement length N_e in determining the rheological characteristics as well as a variety of other mechanical properties like the craze draw ratio, failure mechanisms, and toughness of the polymers. In the original Doi−Edwards model, N_e was envisioned as a phenomenological parameter which represented an effective length of the polymer strand between two entanglement junctions. By adopting this picture, DE could only propose that the entanglement length N_e was independent of the chain length and was purely a property of the entangled chain alone. Indeed, many early comparisons of the DE model relied upon treating N_e as a fitting parameter obtainable from the storage modulus of the material.[3] However, more recently, a surge of interest has arisen to develop models that can delineate the relationship between the entanglement length N_e and the conformational characteristics of the polymer chains (or, more specifically, the characteristic ratio C_∞ of the polymer chain).[5−11] Among these ideas (cf. ref 12 for a recent review of different models proposed for N_e), models invoking *packing* considerations have proven to be quite successful in relating N_e to the molecular features of the macromolecular chains.[5−8,11,13] For instance, the most popular version of this approach[11,13] relates N_e to the volume occupied by the polymer by postulating that the ratio of the volume of space pervaded by a chain of length N_e to its hard-core volume to be a universal constant (of the order 10). Since the volume occupied by a subsegment of a given specific polymer can be quantified from atomistic molecular simulations, an inversion of such a relationship serves as an unambiguous link between N_e and the conformational features of different polymeric materials. By extensive comparisons to the experimental literature, Fetters and co-workers[13,14] have demonstrated that this model can correlate the entanglement molecular weights of a wide variety of polymeric materials. Presently, Doi−Edwards theory in conjunction with the packing models serve as one of the most accurate approaches to link the molecular details of a polymer melt to its macroscopic response and properties (alternative viewpoints of entanglements have also been proposed; cf. for instance refs 12 and 15).

Many recent applications of polymers have however involved multicomponent mixtures of polymers and/or multiblock copolymers.[16,17] For instance, blends of polymeric materials have long served as a popular means to achieve a desirable combination of properties in applications. More recently, the morphological self-assembly patterns exhibited by block copolymers have attracted considerable interest due to the possibility of achieving well-defined long-range order with continuously tunable length scales. The widespread utilization of such materials has raised a number of fundamental

10.1021/ma020930y CCC: $22.00
Published on Web 10/26/2002

questions pertaining to the validity and the extension of the concept of entanglements to such systems.[18] Such issues arise mainly from the fact that most applications utilizing such multicomponent materials involve a heterogeneous, inhomogeneous distribution of the different components and hence are also characterized by distinctly different chain conformations compared to a homogeneous melt. For instance, a number of theoretical and experimental studies have demonstrated that the incompatibility and incompressibility conditions force the statistics of the chain conformations near polymer interfaces (both polymer−polymer and polymer−solid interfaces) to differ markedly from that in the bulk.[19−22] Similarly, block copolymer chains have been demonstrated to adopt stretched non-Gaussian conformations in the microphase separated mesophases.[23] It is however not evident whether the entanglement length N_e of the chains in such inhomogeneous regions are any different from those in the bulk and if so on how to define and/or determine it. On the other hand, a knowledge of this "inhomogeneous" N_e has been claimed to be relevant to a number of macroscopic rheological as well as mechanical properties of these multicomponent systems.[18] Since such issues dominate the processing of these materials, a systematic examination of the concept of entanglements and entanglement lengths in inhomogeneous systems is expected to have significant ramifications in applications involving multicomponent polymers.

To our knowledge, only few previous studies have examined the question of entanglements and the entanglement length of inhomogeneous systems and the explicit relationship, if any, to that of homogeneous polymeric materials. Brown and Russell[18] were one of the first authors to highlight the importance of modified conformations of chains near a polymer−solid interface. They provided qualitative arguments suggesting that the compression of the chains near the interface can profoundly influence the entanglement length by an increase of up to 4 times its bulk value. Further, they claimed that such an increase might in turn help rationalize a variety of unresolved experimental observations relating to the mechanical properties of such polymeric systems. Murat and co-workers[24] utilized molecular dynamics simulations to examine the self-diffusion of block copolymers in lamellar phases. They noticed a significantly high (lateral) mobility of the block copolymer chain, over and above that observed in a homogeneous melt, and concluded that the chains in the lamellar phases exhibit an enhancement in the value of the entanglement length compared to those in a homogeneous melt. (Equivalently, they claimed that the number of entanglements was lower in the inhomogeneous phase.) In contrast, Pan and Schaffer[25] undertook a kinetic Monte Carlo simulation of self-diffusion in block copolymers and used an indirect approach to deduce that the accompanying inhomogeneity and the anisotropic chain conformations had no perceptible influence on the entanglement lengths of the chains in lamellar phases. While the arguments of Brown and Russell pertained specifically to polymer interfaces, it proves an easy task to extend their reasoning to diblock copolymers to compare with the above simulations. Indeed, such an objective can be realized by drawing an analogy between the conformations of the chains in a lamellar block copolymer and those in homogeneous melts of stiff chains.[26] Several experiments have demonstrated that the latter system possesses lower entanglement molecular weights than the corresponding flexible systems. These results have been rationalized as arising due to the increased "exposure" of the stiff chains to the other chains which allow for an enhancement in the topological constraints faced by the chains. Chains in a lamellar block copolymer are stretched, and therefore one might also expect that the entanglement length of such chains be lower than the value corresponding to that of a homogeneous melt—a result which contradicts with the simulation studies discussed above.

In the present research, we present a systematic examination of the concept of entanglements (both inter- and intraspecies) in multicomponent polymeric systems with an emphasis on the role of inhomogeneity and its quantitative influence. We believe that the shortcomings of the above theoretical studies and the contradictory results can be traced to the utilization of a dynamical approach to determine the entanglement length N_e, which is fundamentally a topologically determined equilibrium quantity. Inspired by the successes of the packing models for a wide range of situations,[11,13,14] we propose that the essential idea behind the concept of an entanglement is universal and independent of the presence of inhomogeneities. However, we claim that an appropriate adjustment to the actual measure of this entanglement, N_e, can arise due to changes in the statistics of the chain conformations accompanying such inhomogeneous situations. It is of course not obvious whether indeed the "static" inhomogeneous entanglement length will serve the same role in dynamics of inhomogeneous systems as played by the conventional homogeneous N_e. Such a question can be resolved only by developing an appropriate dynamical theory of inhomogeneous concentrated polymeric systems,[27] which is still a direction of active research in many groups including ours. However, even in the absence of such a theory, we believe that it is of utility to delineate the manner in which the inhomogeneity and the changes in the chain statistics influence the behavior of this static entanglement length. Such results might provide useful information to interpret experiments pertaining to the strength and cohesion of the interfaces and the high-strain properties of the materials as well as aid in the development of theoretical models which can provide a satisfactory description of the dynamics in such systems.

In this research we undertake to calculate the entanglement lengths in inhomogeneous systems by adapting the packing models for entanglements. As mentioned earlier, a variety of different (and somewhat equivalent) models have been proposed within these packing approaches. In this research we utilize the specific framework proposed by Kavassalis and Noolandi (KN)[6−8] which lends itself to a relatively straightforward implementation by Monte Carlo techniques. Our choice of the KN model is also motivated by some of the physical implications embedded therein, which, as we discuss later in the text, permits us to calculate quantities such as interpenetrating entanglements. However, we also demonstrate that the qualitative features of the results we obtain transcend the framework we employ and are equivalent to those obtained by employing other packing models. In this article we focus mainly upon our results obtained in the contexts of polymer−polymer interfaces. In addition to delineating the effects of inhomogeneity, we also provide

some qualitative arguments to deduce the implications of our results for the contexts of experimental and theoretical studies of the mechanical properties of such systems.

The outline of the rest of article is as follows: In the next section we outline the salient features accompanying the KN model of entanglements we have chosen. In section III, we describe in brief the elements of self-consistent-field theory and the manner in which such a theory enables one to compute the quantities present in the entanglement model. Section IV details the main features of the simulation techniques we employ in solving the self-consistent-field equations and in performing the Monte Carlo statistics. In section V, we outline our results obtained for polymer blends. Our presentation focuses on two quantities: the entanglement length in inhomogeneous situations and the degree of interpenetration between different polymeric components. In section VII, we argue that the latter can serve as a measure to quantify the slip as well as the toughness of polymer interfaces. Our main motivation in presenting these results (which is mostly on a speculative level) is to provide experimental means to test the concepts and the results presented in this article. In section VIII, we summarize our findings with an outlook for future work.

II. Kavassalis−Noolandi Concept of Entanglements

In this research we utilize the definition of an entanglement as proposed by Kavassalis and Noolandi (KN) to delineate the behavior of the entanglement lengths in inhomogeneous polymeric systems. Our choice was dictated by the fact that the KN definition relates the concept of "entanglements" to the qualitative picture of "constraints" (see below) and thereby allows one to determine for instance the degree of entanglements arising between different components in a multicomponent mixture. In contrast, such computations cannot be afforded straightforwardly by some of the other successful packing models for entanglements. However, to demonstrate the equivalence of the different approaches, in section VI we provide an explicit comparison of the results obtained from the KN definition of entanglements with those obtained by employing the packing factor approach proposed by Fetters and co-workers.[11] In this section, we describe in brief the essential idea behind the Kavassalis and Noolandi definition of entanglements. A reader interested in an elaboration of the details (including applications to polymer solutions) is advised to refer to the original articles.[6−8]

The seminal works of Kavassalis and Noolandi (KN) replaced the concept of a chain length (denoted N in the following) independent entanglement length N_e by a chain length dependent new parameter termed as the *coordination number*. The latter, denoted as $\bar{N}$, was meant to characterize (in an averaged manner) the number of effective constraints imposed by the polymeric matrix on a subsegment of a test chain. Explicitly, if we consider an elemental volume V'_e enclosing N'_e segments of a test chain (cf. Figure 1), the coordination number $\bar{N}(N'_e)$ is then defined as

$$\bar{N}(N'_e) = \frac{1}{N'_e}\sum_{m=1}^{N} S_{\text{nontails}}(m)m \qquad (1)$$

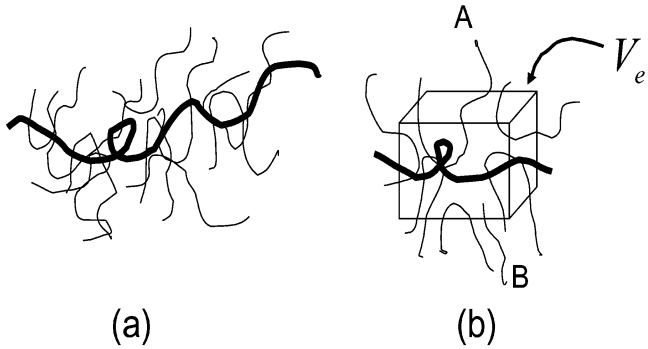

Figure 1. (a) A pictorial depiction of an entangled melt. The highlighted chain represents the test chain for which the number of constraints are computed. (b) A representation of the elemental volume V_e containing N_e segments of the test chain. $S(m)$ embodies the statistics of the size of the loops (denoted as A) and free ends (denoted as B) of other chain segments present in this volume.

In the above equation, the quantity $S_{\text{nontails}}(m)$ denotes the average number of other nontail polymer segments (cf. Figure 1) with a length of exactly m units in the elemental volume V'_e. This quantity can be viewed as a measure of the number of effective constraints of length m (a free end is not construed as an effective constraint) imposed by the other chains on the test chain. As stated in the form embodied in eq 1, the coordination number $\bar{N}$ represents a quantity that is completely specified by the statistics of the chain conformations (which determine $S_{\text{nontails}}(m)$) and N'_e and is unrelated to the entanglement length N_e. However, KN utilized this parameter in an ingenious manner by postulating that the coordination number $\bar{N}$ defining the entanglement length N_e is a universal quantity (denoted $\bar{N}^*$) independent of the specific nature and the conformational features of the polymer. Given this universal value for $\bar{N}^*$, an inversion of eq 1 thereby provides an unambiguous definition for the entanglement length for specific polymeric systems. Kavassalis and Noolandi provided an extensive survey of the experimental literature to support their claim that indeed $\bar{N}(N_e)$ can be treated as a universal constant for different polymeric systems. Furthermore, they also demonstrated that this assumption allowed one to predict the concentration scaling of the entanglement lengths in polymer solutions which were in reasonable agreement with the experimental results.

In this research, we postulate that the above proposals of KN are universal and hence are equally applicable to inhomogeneous situations. With this underlying premise, we utilize the definition of the coordination number $\bar{N}$ and its relationship with N_e to determine the manner in which the changes in the conformational characteristics which accompany inhomogeneous systems impacts upon the value of N_e. However, a rigorous implementation of the KN definition proves to be an onerous task due to the inversion of eq 1 entailed in such an approach. To circumvent this difficulty, we adopt a different strategy whereby we compute for inhomogeneous situations the number of effective constraints ($\bar{N}$) experienced by a subchain with a length equal to that of the entanglement length of a homogeneous melt. If indeed the entanglement lengths in an inhomogeneous phase were identical to that in a homogeneous phase, one would correspondingly expect that the number of constraints $\bar{N}$ be unchanged. On the other hand, a decrease (increase) in the number of constraints

would indicate an increase (decrease) in the effective entanglement lengths. This approach, albeit indirect, allows us to document in an efficient and quantitative manner the interplay between the entanglements and the chain conformational statistics. Furthermore, it is useful to reiterate the physical picture wherein the entanglement length is but a mere fictitious representation of the constraints faced by a chain. Consequently, we believe that a quantification of the "number of constraints" as embodied by the coordination number $\bar{N}$ is more representative of the physical situation than the quantitative value of the entanglement length.

In the next section we outline the details of self-consistent-field theory which allows the enumeration of $S(m)$ for inhomogeneous polymeric systems.

III. Self-Consistent-Field Theory

To adapt the KN definition of entanglements to the situation involving multicomponent polymer mixtures, one needs an approach to determine the conformational statistics (as embodied in $S_{\text{nontails}}(m)$) of the system of interacting polymer chains. We adopt the polymer self-consistent-field theory (SCFT) to enumerate the conformational features of the system of interacting polymer chains. Since many recent articles have reviewed in detail the concepts embodied in SCFT,[28−30] in the following we restrict the discussion to a brief overview of the approach. In a nutshell, polymer SCFT enumerates the statistical features of the interacting system of polymer chains by considering an equivalent system of noninteracting chains in the presence of pseudochemical potential fields.[31,32] Such a procedure is enabled by employing field−theoretic techniques, which can be used to demonstrate that that the thermodynamics of the system of noninteracting chains serves as a mean-field approximation to the thermodynamics of the system of interacting chains.[29] SCFT further specifies that these chemical potential fields are to be determined in a self-consistent manner so as to impose the inhomogeneous densities of the appropriate components. For instance, in the case of A + B polymer blends and AB diblock copolymers, the interactions are replaced by two spatially inhomogeneous chemical potential fields, denoted typically as $W_+(\mathbf{r})$ and $W_-(\mathbf{r})$, which serve to impose the incompressibility criterion and the difference in the local densities of the A and B components. Explicitly, $W_-(\mathbf{r})$ and $W_+(\mathbf{r})$ are postulated to be the solution of

$$W_-(\mathbf{r}) = 2\chi N[\phi_A(\mathbf{r}) - \phi_B(\mathbf{r})] \tag{2}$$

and

$$\phi_A(\mathbf{r}) + \phi_B(\mathbf{r}) = 1 \tag{3}$$

[note that (3) represents an implicit equation for $W_+(\mathbf{r})$[29]] wherein χ denotes the usual Flory−Huggins parameter describing the strength of A−B monomer interactions, and the fields $\phi_A(\mathbf{r})$ and $\phi_B(\mathbf{r})$ represent the nondimensionalized density fields of the A and B components. The above equations are converted to a self-consistent condition by requiring that the density fields $\phi_A(\mathbf{r})$ and $\phi_B(\mathbf{r})$ be obtained from the statistics of the noninteracting chains in the external fields $W_+(\mathbf{r})$ and $W_-(\mathbf{r})$. The main simplification which ensures the success of this method arises from the fact that the statistics of a polymer molecule in an external field is completely specified by solving a diffusion equation for its distribution functions.[31,32] For instance, for a polymer chain under the action of an external field $U(\mathbf{r})$, if $q(\mathbf{r},s)$ denotes the probability that a section of chain of contour length s and containing a free end has its "connected end" at $\mathbf{r}$, then it can be shown that $q(\mathbf{r},s)$ satisfies

$$\frac{\partial q}{\partial s} = \nabla^2 q - U(\mathbf{r})\, q(\mathbf{r},s); \quad q(\mathbf{r},0) = 1 \tag{4}$$

Further, the density field $\phi(\mathbf{r})$ of the polymer can be expressed in terms of $q(\mathbf{r},s)$ as

$$\phi(\mathbf{r}) = \mathcal{C}\int_0^N \mathrm{d}s\; q(\mathbf{r},s)\, q(\mathbf{r},N-s) \tag{5}$$

where $\mathcal{C}$ is a constant arising from the nondimensionalization of the equations. Similar diffusion equations and relationships can be derived in the case of diblock copolymeric systems and polymer blends (cf. ref 29 for more details) to furnish the self-consistent equations for the $W_-(\mathbf{r})$ and $W_+(\mathbf{r})$.

A number of approaches have been proposed to solve the self-consistent equations for the potential fields and to thereby determine the compositional profiles characterizing the inhomogeneity.[33,34] In this work, we adopt the approach put forth by Drolet and Fredrickson[34] which employs a simple dynamical prescription which relaxes to the solution of the self-consistent equations. This approach has been used with success in a wide variety of situations involving multicomponent block copolymers,[34] blends of block copolymers with homopolymers, thin films of polymers,[35] block copolymer−nanoparticle blends, etc.[36] As an illustration of this approach in the context of the present research, Figure 2a,b depicts the composition profiles in a segregated polymer blend and a lamellar diblock copolymer obtained by using this technique.

IV. Simulation Approach

We adopt a lattice model of the polymer to enumerate the statistics of the constraints experienced by a chain. In this article, our considerations are restricted to polymer melts, and therefore the effects arising from excluded-volume interactions are ignored. In such a situation, an enumeration of the polymer configurations in a homogeneous melt can be effected by a mapping onto the statistics of unbiased self-intersecting random walks on a lattice. To accomplish this objective, we employ a three-dimensional cubic lattice with a lattice spacing corresponding to the Kuhn segment length of the polymer. Polymer conformations are then generated by "growing" the chains through random walks on this lattice. The main advantage of such a technique is the ease with which this procedure can be generalized to account for the presence of inhomogeneous phases. Explicitly, in such situations, the previously computed self-consistent potentials act on the polymer, and the statistics of the chain conformations are now described by a mapping onto biased (arising from the self-consistent potentials) self-intersecting random walks.

Preliminary to an exposition of the simulation approach we adopt, we describe the methodology utilized by KN to compute the coordination number in the context of a homogeneous melt of noninteracting polymer chains.[6−8] In the present research, this quantity also serves as a reference to base our comparisons of the effects arising from compositional inhomogeneities.

To enable a computation of $\bar{N}$ for homogeneous melts, we consider a cubic volume of size V_e (i.e., with sides $V_e^{1/3}$) centered at a position **r**. The volume V_e represents the average volume pervaded by a chain segment of size N_e and is chosen on the basis of an independent simulation which grows random walks with N_e steps starting from **r**. (For a homogeneous melt, the location of the position **r** is redundant. However, we retain the reference to this positional coordinate since it enables an easier description of the modifications entailed by the inhomogeneous situation.) The latter enables one to discern the mean-squared displacement of such random walks which is then utilized to deduce the sides of the cubic volume. In view of the lattice approach we have adopted, the sides of cubic volume were chosen to be the closest possible integer multiple of a Kuhn segment length of the polymer. To enumerate $S_{\text{nontails}}(m)$, a monomer is chosen randomly within the chain and is then placed in a random location within this cube. Subsequently, the polymer conformations are grown randomly in both directions (i.e., toward the first and the last unit of the polymer) until the random walk either escapes from the cubic volume or terminates due to reaching the free end. In the event that the random walk is not a part of the free end, we count the number of segments of the walk present within the volume and update $S_{\text{nontails}}(m)$ accordingly. This procedure is repeated for different choices of the monomers as well as at different randomly chosen locations within the cube (our simulations typically involved statistics collected using 10^7 such walks), at the end of which a rescaled $S(m)$ is determined by normalizing the first moment of the number of walks to the total number of lattice points enclosed by the cube. A knowledge of the distribution $S_{\text{nontails}}(m)$ in conjunction with eq 1 then allows us to compute the coordination number $\bar{N}$.

Two main features distinguish the situations of interest in this article from that discussed above: (i) Because of the inhomogeneous composition profiles, the statistics of the random walks are biased by the potential field and hence are no longer spatially isotropic. For instance, the role of the interface of a polymer blend can be likened to that of a reflecting surface which prevents the excursions of chains from one phase into the other (such an analogy being valid only in the limit of strong incompatibility). Consequently, the statistics of the chains near the interface of a polymer blend are expected to be anisotropic in the direction normal to the interface. Such features manifest in the computation of the size of the elemental volume V_e containing N_e monomers of the chain. Explicitly, in inhomogeneous phases such as polymer blends, the elemental volume V_e is in general an anisotropic and a spatially dependent quantity. (ii) The monomers can no longer be chosen at random to be placed inside the elemental volume. Instead, the monomers now possess a distribution of probabilities specifying their likelihood of being found at a position **r**. For instance, the probability of finding the link of a block copolymer is highest at the boundaries of the lamella and diminishes as one moves inside the lamella. As an indirect consequence of this feature, the statistics of the free ends also possess an inhomogeneous distribution (in contrast to a homogeneous melt).

We account for the above features by modifying the simulation approach adopted by KN. At the outset, we enumerate the statistics of random walks of N_e segments which are centered at **r**. This is accomplished by placing a randomly chosen monomer s at the position **r** and then growing a chain of N_e segments. However, in contrast to the previously described situation, the random walks are now biased by the self-consistent potential whose value at a specific location is determined by both the identity of the monomer (i.e., the species to which it refers) at that location and its spatial coordinate. In addition, the statistics of the biased random walks are also assigned weights to account for the inhomogeneous distribution of the monomers. Explicitly, a random walk which starts with the monomer s at the position **r** and ends with the monomer $s + N_e$ at the position **r′** is assigned a weight:

$$w = q(\mathbf{r},s)\, q^{\dagger}(\mathbf{r}',s+N_e) \tag{6}$$

In the above equation, $q(\mathbf{r},s)$ carries the same interpretation as the quantity defined by eq 4 and represents the probability that a section of chain of contour length s and containing a specified free end has its "connected end" at **r**. The quantity $q^{\dagger}(\mathbf{r},s)$ denotes the conjugate distribution function which describes an analogous probability distribution with respect to the other free end of the chain. The numerical values of both these quantities are specified by diffusion equations similar to eq 4 and can be calculated once the self-consistent potential fields are specified (cf. ref 29 for details). By repeating the above procedure by starting with different randomly chosen monomers, we deduce the sides of the elemental volume V_e (which is in general an orthogonal parallelepiped). Thereafter, the enumeration of $S_{\text{nontails}}(m)$ proceeds in a manner similar to the case of a homogeneous melt. At a location **r**, the elemental volume is chosen on the basis of the previously enumerated statistics of the random walks starting at that location. Polymer conformations are then grown starting from random points inside this cube through biased random walks toward the first and the last units of the chain. In line with the approach adopted above, a random walk which starts with the monomer s at the position **r′** is assigned a weight,

$$p = q(\mathbf{r}',s)\, q^{\dagger}(\mathbf{r}',s) \tag{7}$$

Such an enumeration procedure allows us to determine $S_{\text{nontails}}(m)$ and therefore the coordination number $\bar{N}(\mathbf{r})$ which, in view of the inhomogeneity, is an explicit function of the positional coordinate **r**.

In the following sections, we discuss the results obtained by applying the above-described procedure to the specific cases of symmetric polymer blends. As mentioned earlier in the text, our simulations are effected by fixing the entanglement length N_e to probe the changes in the coordination number $\bar{N}$ (which tracks the number of constraints experienced by a chain) which arise as a result of the changes in the conformational characteristics in inhomogeneous phases. In the present article, we focus on the universal nature of $\bar{N}$ and are mainly interested in the qualitative features arising from the compositional inhomogeneities. Consequently, we choose an artificial N_e and employ it as a baseline value to discern the effects of compositional inhomogeneities. The results described in the following sections were all obtained using a value of $N_e = 27$. The effects arising from varying the entanglement length N_e, albeit interesting, prove computationally expensive. Consequently, we eschew these considerations in this pre-

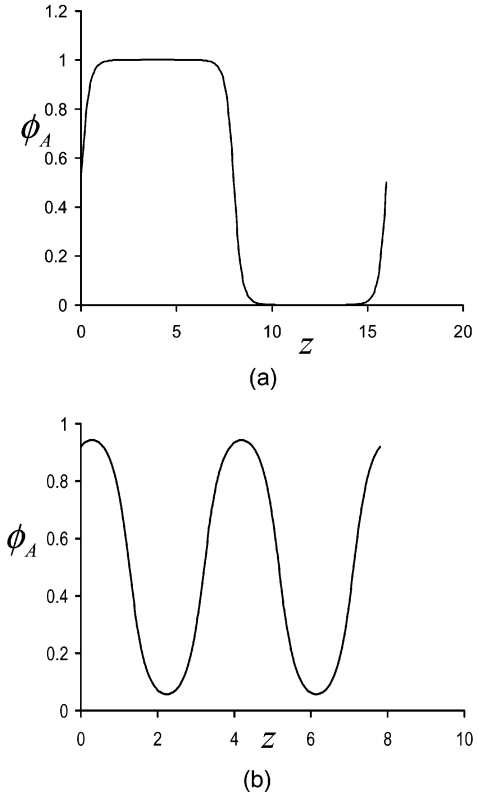

Figure 2. Density profiles calculated utilizing Fredrickson–Drolet numerical scheme for the solution of SCFT equations. (a) A symmetric A + B polymer blend with $\chi_{AB} = 1.1 \times 10^{-2}$, $\chi N = 8.0$. (b) A symmetric AB diblock copolymer with $\chi N = 15$.

liminary report. Furthermore, the results outlined are restricted to a single chain length, $N = 1000$. Variations in N do cause minor variations in the number of constraints experienced by a chain. However, we have verified that the qualitative features of our results are unchanged by such variations. For the above set of parameters, the coordination number of a bulk melt is $\bar{N} = 7.78$. Note that our choice of $\bar{N}$ (and N_e) is chosen primarily to ensure efficient simulations.

V. Entanglement Lengths near the Interface

As noted in the preceding section, the statistics of random walks in inhomogeneous multicomponent polymeric systems are explicitly dependent on both the identity of the monomer and its position. Consequently, identical sized segments of A and B chains which are centered at the same position could in general have completely different statistics and sizes. Therefore, in the case of a polymer blend, one can define two distinct sets of coordination numbers: $\bar{N}_A(\mathbf{r};N_e)$, which represents the coordination number of an A chain of length N_e which is centered at the position $\mathbf{r}$, and $\bar{N}_B(\mathbf{r};N_e)$, representing the coordination number of a B chain of length N_e centered at the position $\mathbf{r}$. Further, given the values of these two coordination numbers, one can define an "average" coordination number as

$$\bar{N}(\mathbf{r}) = \phi_A(\mathbf{r})\, \bar{N}_A(\mathbf{r};N_e) + \phi_B(\mathbf{r})\, \bar{N}_B(\mathbf{r};N_e) \qquad (8)$$

where $\phi_A(\mathbf{r})$ and $\phi_B(\mathbf{r})$ denote the volume fractions of the A and B species at the position $\mathbf{r}$. We would like to stress that the above definition of an averaged coordination number does possess a certain degree of arbitrariness

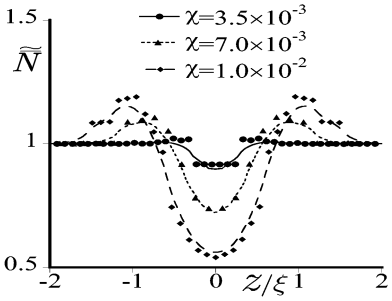

Figure 3. Variation of the nondimensionalized coordination number $\tilde{\bar{N}}$ (explicitly, $\tilde{\bar{N}} \equiv \bar{N}(\chi)/\bar{N}(\chi=0)$) as a function of the distance from the interface z. The latter is nondimensionalized by the interface width ξ. The points are the simulation results, and the curves are drawn as a guide to the eye. Polymer mixtures with different degrees of incompatibility are displayed. (a) Weak incompatibility: $\chi = 3.5 \times 10^{-3}$. (b) Intermediate level of incompatibility: $\chi = 7 \times 10^{-3}$. (c) Strongly incompatible mixtures: $\chi = 1 \times 10^{-2}$.

and that other equally reasonable "mixing rules" can be proposed. However, we chose the above definition since it conforms closest to the KN picture wherein the coordination number is viewed as a quantification of the number of constraints experienced by a chain. Furthermore, we have also verified by explicit simulations that alternative definitions of the averaged coordination number do not impact upon the qualitative features of the results we present in this section.

In the following, we present results that explicitly demonstrate the changes in the coordination number (and hence the entanglement length) which arise as a result of the changes in the conformational characteristics of the polymer chains. To render the physical implications transparent, we have utilized nondimensionalized quantities, wherein the coordination number $\bar{N}$ is normalized by its value corresponding to a homogeneous polymer melt and is denoted as $\tilde{\bar{N}}$. We choose the Z axis to correspond to the direction normal to the interface and fix the origin of the coordinate system at $z = 0$. In this reference frame, the results from self-consistent-field theory indicate a phase-separated polymer blend mixture with the majority A phase constituting the left side of the interface ($z < 0$) and the B phase the right side of the interface ($z > 0$). We have also nondimensionalized the spatial coordinate z in each situation by the corresponding interfacial thickness ξ. The values of the latter quantity (ξ) are determined by fitting the density profile determined through our SCFT computations to the theoretically predicted profiles.[37]

Figure 3 displays the variation of the nondimensionalized coordination number $\tilde{\bar{N}}$ as a function of the distance from the interface z. From the results depicted, three characteristic zones can be identified:

(i) Bulk Zone. This region occurs at positions far from the interface, wherein the coordination number $\bar{N}$ acquires a value identical to that corresponding to a homogeneous melt. The presence of such a zone can be rationalized by the fact that in polymer blends the effect of the inhomogeneity arising from the phase-separated morphology impacts only upon the conformations of those chains which are present near and in the interfacial zone. In contrast, the regions far from the interface (as quantified by $z/\xi \gg 1$) are characterized by chain conformations which are similar to that in a homogeneous melt of A or a B polymers. Consequently, the entanglement length and the coordination number

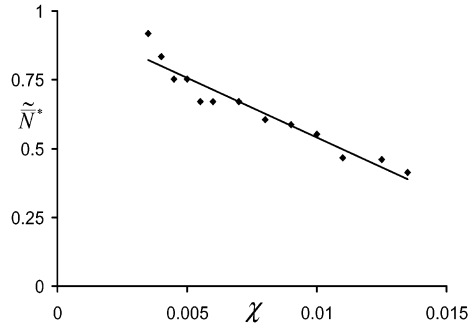

Figure 4. Variation of the minimum values of nondimensionalized coordination number $\tilde{\bar{N}}$, denoted as $\tilde{\bar{N}}^*$, as a function of the degree of incompatibility between the polymers. Also shown is the best linear fit to the data represented by $\tilde{\bar{N}}^* = 0.975 - 43.49\chi$.

of a polymer in this region are also unchanged from its value in a homogeneous melt.

(ii) Interfacial Zone. This region corresponds to the zone adjoining the interface (approximately, in the range $-{}^1/_2 \lesssim z/\xi \lesssim {}^1/_2$) wherein the coordination number displays a reduction compared to its value in a homogeneous melt. Such an effect can be explained on the basis of the conformations of the chain in the interfacial zone. As alluded to earlier, the interface of a strongly incompatible polymer blend can be likened to that of a reflecting solid wall (along with a small degree of attraction, which serves to maintain the incompressibility constraint).[22] Consequently, the chains near the interface are in a state of compression which manifests in a reduction in the volume pervaded by a chain compared to its value in a homogeneous melt. As might be expected, a compressed chain exposes less of itself to the other chains and therefore experiences a reduction in the number of constraints. In turn, such an effect manifests in the reduced values of coordination number displayed in the interfacial zone.

Figure 3 also depicts the explicit effects of the degree of incompatibility upon the reduction in the coordination number at the interfacial zone. It is evident that the degree of reduction of the coordination number increases with an increase in the degree of incompatibility or the segregation of the polymers. Indeed, the situation corresponding to weak incompatibility ($\chi = 3.5 \times 10^{-3}$) exhibits only a 16% reduction in the coordination number in contrast to an almost 45% decrease seen in the case of strongly incompatible mixtures ($\chi = 1 \times 10^{-2}$). The qualitative arguments expounded in the preceding paragraph allow us to rationalize these effects as an explicit manifestation of the reduced degree of compression (and changes in the conformational characteristics) that accompany a weakly incompatible polymer melt. In Figure 4 we depict the results of a more systematic exploration of this effect by displaying the variation of the minimum values of the coordination numbers as a function of the degree of incompatibility between the two components. It is indeed seen that the degree of incompatibility exercises a profound influence on the reduction in of the coordination number. Explicitly, an increase in the incompatibility leads to a decrease in the coordination numbers and hence an increase in the entanglement lengths at the interface. Furthermore, the inset to Figure 4 demonstrates that the variations of the coordination number in this limited range of incompatibility can be fitted to a linear fit of the form $\tilde{\bar{N}}^* = 0.975 - 43.49\chi$. As is intuitively evident, the limit of $\chi = 0$ corresponds to a compatible, symmetric mixture wherein we expect the coordination numbers (and the entanglement lengths) to be unmodified from its bulk, homogeneous values (i.e., $\tilde{\bar{N}}^* \simeq 1$). On the other hand, for $\chi \simeq 0.0224$ wherein $\tilde{\bar{N}}^* \simeq 0$ can be considered as the limit wherein the polymers become incompatible.[18] Note however that our results are explicitly dependent on the value of N_e chosen for the simulations and are not universal.

Previous researchers[18,38] have speculated that the changes in the conformations that accompany a polymer chain near the interface of a polymer blend can lead to a corresponding increase in the entanglement length in such situations. To our knowledge, the results embodied in Figures 3 and 4 constitute the first systematic and quantitative evidence for this effect. However, it is of more interest to probe the manner in which the effects on the coordination number $\bar{N}$ manifests itself on the entanglement length N_e. In principle, such an objective can be realized by taking recourse to and inverting the relationship existing between $\bar{N}$ and N_e as embodied by eq 1 and the universality postulate of KN. However, the lattice model we have chosen for our model renders this procedure ineffectual and inaccurate by constraining the changes in the entanglement lengths to discrete values corresponding to changes in the size of the segmental volume. A more accurate approach invoking a continuum model with a spherical or ellipsoidal elemental volume might possibly capture the continuous changes in the entanglement lengths. In the absence of such a model, we provide some qualitative scaling-based arguments to suggest the magnitude of the variations entailed in the entanglement length: Our arguments specifically focus on the statistics of the conformations of the chains and their relationship to the number of segments. In a homogeneous melt, a strand of a flexible polymer chain containing N_e segments occupies an elemental volume $V_e \sim N_e^{3/2}$. To a good degree of approximation (see also section VI), the number of constraints experienced by a section of the chain can be expected scale with this volume, and hence $\bar{N} \sim N_e^{3/2}$. Consequently, if some region of the melt has a lower coordination number, denoted as $\bar{N}'$, then the entanglement length corresponding to this region scales as $N_e' \sim N_e(\bar{N}/\bar{N}')^{2/3}$. On the basis of our simulations, we have verified that this scaling law is indeed reasonably obeyed in the context of homogeneous melts. However, the situation considered in this article pertains to inhomogeneous situations and specifically to effects arising from the non-Gaussian statistics of the polymer chains. In fact, we have argued that the reduction in the coordination numbers is mainly a manifestation of the compression of the chains near the polymer blend interface. In such situations, it is more reasonable to expect $V_e \sim N_e^{1+\beta}$, where $\beta < {}^1/_2$. Indeed, on the basis of the consideration of the potential experienced by the chain (depicted in Figure 5), one might expect that short enough segments of the chain near the interface (the position denoted as Z_1^* and the chain denoted as C_1 in the figure) will be confined to the potential well, and therefore the situation at hand might correspond more closer to the limit $\beta \ll {}^1/_2$. With this modified scaling form for the elemental volume, we obtain $N_e' \sim N_e(\bar{N}/\bar{N}')^{1/(1+\beta)}$. This suggests that the decreases in the coordination numbers displayed by Figure 4 can profoundly influence the entanglement length of the polymer chains near the interface. Moreover, our qualitative scaling

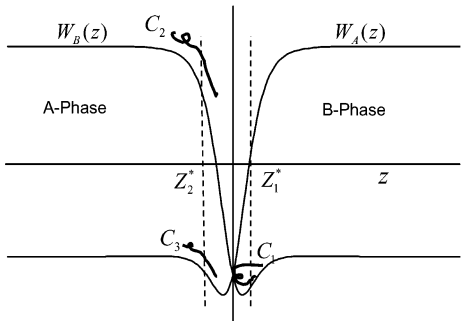

Figure 5. A depiction of the inhomogeneous self-consistent potential fields acting on the A monomers (denoted as $W_A(z)$) and B monomers (denoted as $W_B(z)$) for the situation wherein the majority A phase is to the left of the interface ($z < 0$). The symbols Z_1^*, Z_2^*, C_1, C_2, and C_3 are discussed in the text.

arguments suggest that these effects can be as significant so as to lead to almost a doubling of the entanglement length (in the limit $\beta \simeq 0$).

(iii) Intermediate Zone. While the presence of a bulk and an interfacial zone were anticipated by previous researchers, the existence of a third, intermediate zone has not been suggested prior to this research. This region, which exists between the interfacial and bulk zone, is characterized by an increase in the coordination number or, in other words, a decrease in the entanglement length! The existence and the features of this zone can be rationalized as arising from two sources, the characteristics of both of which are captured by the self-consistent potential field (which manifests directly in the chain conformations). Figure 5 displays the SCFT-based potential field corresponding to a strongly incompatible polymer situation. It is seen that the potential field displays a steep barrier followed by a nonzero, albeit weak, potential well. The former characteristic is a manifestation of the incompatibility of the polymers and serves as the reflecting surface alluded to in our discussion of the interfacial zone. The presence of the potential well results from the incompressibility constraint which strives to maintain a constant density throughout the system. If we focus on the particular point denoted as Z_2^* in the figure, it is evident that the gradients of the potential fields acting at Z_2^* tends to stretch both A and B chains (denoted as C_3 and C_2, respectively) toward the interface. The former arises as a result of repulsion from the B phase, while the latter arises as a result of the attraction toward the potential well. We believe that this stretching of the chains (leading to an increase in the effective volume of the chain, whence suggesting $\beta > {}^1/_2$) manifests in the increase in the coordination number. Indeed, as one might expect, the effect of this stretching diminishes as the polymers become more compatible and in fact vanishes in the situations accompanying weakly incompatible polymers ($\chi = 3.5 \times 10^{-3}$). Another limit wherein this zone is expected to vanish corresponds to the situation involving polymers with long entanglement lengths—in which case the statistics of segments of the chain can be dominated by the compressing effects of the interfacial zone.

In summary, the above discussion delineates in a quantitative and systematic manner the variations in the coordination number and the entanglement lengths as a function of the distance from the interface. Our results highlight the profound influence exerted by the changes in the chain conformations (which accompany inhomogeneous situations) upon the number of constraints experienced by a chain. Further, our results also suggest an important role for the degree of incompatibility between the polymers in determining the magnitudes of this influence. Indeed, we have demonstrated by a combination of both numerical results and scaling arguments that the limit of strong incompatibility could result in effects leading up to a doubling of the entanglement length near the interface. In the following section, we discuss the ramifications of the above results upon experiments measuring the mechanical and rheological properties of the polymers.

VI. Comparison to Other Packing Models

The research presented in the previous section employed the specific packing model of Kavassalis and Noolandi to account for the inhomogeneities in entanglements. However, as we mentioned in the Introduction, a variety of alternative approaches have also been proposed to relate the packing and the conformations of the chains to the entanglement length N_e.[5,9,11] Our primary motivation in adopting the KN model was to exploit the physical picture embodied therein, enabling one to compute quantities such as the degree of interpenetration (see next section). In contrast, most of the other packing models quantify the entanglement length purely based on the volume pervaded by the chain and hence do not afford a straightforward computation of entanglement related interpenetrations. It is however of interest to probe the manner in which the average entanglement length as derived utilizing the KN framework relates to that computed using other packing models. Indeed, a successful correlation between the results from different approaches would serve to establish their equivalency and thereby also add support to the utility of such packing models for situations involving inhomogeneous compositions.

To achieve the above objective, we have utilized the Fetters's model of entanglements in conjunction with our simulation approach.[11,13,14] In Fetters's approach, the entanglement length N_e is quantified in terms of a phenomenological entity termed as the packing parameter. This parameter (denoted as $\bar{p}$) is defined as the ratio of the volume pervaded by the chain to the hard core volume of the chain. Similar to the approach adopted by KN, an implicit relationship between $\bar{p}$ and the entanglement length N_e is proposed by postulating that the value of the packing parameter corresponding to a chain strand of entanglement length is a universal constant (of the order 10) and independent of the specific details of the polymer chain involved. Figure 6 displays an explicit comparison between the entanglement lengths as derived from the KN model and the Fetters's packing approach. In lieu of determining the entanglement lengths, we have chosen to display the results in terms of the variations of a normalized packing parameter $\tilde{p}$ and a normalized coordination number $\tilde{N}$. It is evident from the results depicted that both the quantitative values as well as inhomogeneity influenced spatial variations display identical behavior in both these parameters. On the basis of the obvious similarities between the KN approach and the Fetters's model, one might have indeed speculated that the packing parameter and the coordination numbers embody the same physical concepts, albeit in different quantitative forms. Indeed, such a relationship can be rendered explicit if the total number of constraints experienced

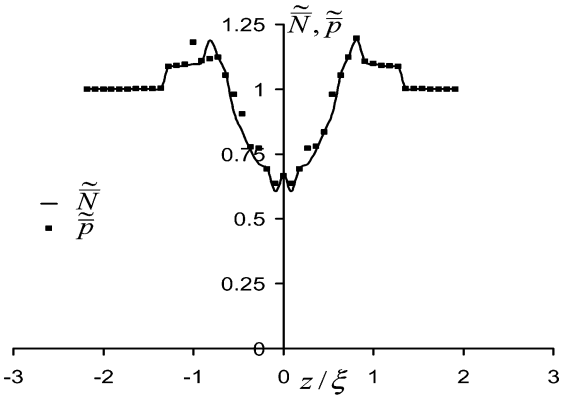

Figure 6. Variations of the nondimensionalized coordination number $\tilde{\bar{N}}$ and the packing factor $\bar{p}$ across the interfacial region ($\chi = 8 \times 10^{-3}$). Both quantities are nondimensionalized by their values in the homogeneous melt.

by a chain can be proved to scale as the volume pervaded by the chain. While we are not aware of any theoretical approaches that have probed such a relationship, our results presented in Figure 6 demonstrate the validity of this empirical proposal even for situations involving inhomogeneous compositions. In sum, the results presented in this section suggest that our discussions in the preceding sections are independent of the specific framework we had adopted to compute the inhomogeneous entanglements.

VII. Interpenetrating Entanglements at Interfaces

Over the past decade, several experimental and theoretical researchers have advanced phenomenological models correlating the total number of interfacial entanglements as well as the interfacial entanglement length to mechanical properties.[39−41] For instance, the failure mechanisms of a polymer−polymer interface has been successfully described by a generalized phase diagram with interfacial stress and the density of interfacial entanglements as the governing variables.[42] Further, models have been proposed relating mechanical properties like the cohesive toughness, craze draw ratio, and the interfacial slip to the number of entanglements in a polymer−polymer interface. However, as we mentioned earlier in the text, most of the models developed so far have not accounted for the effects arising from the variations in the entanglement lengths across the interface. In addition, most of these models have also relied upon the classical picture wherein the entanglements are typically viewed as stress supporting binary "junctions". Given the widespread interest in quantifying the interfacial entanglements, it is natural to query "what, if any, are the effects of the inhomogeneities predicted in the present research upon the mechanical and rheological properties of polymer−polymer interfaces?" To answer such a question, one would need to develop microscopic models that can embody the concept of an inhomogeneous distribution of constraints, a task that is beyond the scope of this article. In the absence of such a theory, we offer some speculative comments and numerical results on some of the implications arising from the framework and the results of this research. We would like to stress the qualitative nature of our arguments and the fact that it is not backed by extensive experimental comparisons. By detailing our ideas, we are hoping to spur experiments that can potentially validate or invalidate the nonclassical approach we have adopted in this research.

A. Slip in Polymer Interfaces. Recently, there has been much interest in understanding and quantifying slip in polymeric materials.[39,41,45] The term "slip" has been employed to denote a generic situation wherein the polymeric material responds in a nonuniform manner to an imposed shear stress. Such effects can arise either during the interaction of polymers with solid surfaces or due to the interactions between two incompatible polymers.[45,46] Examples of the latter include slip phenomena at the polymer interfaces in a blend, formation of slip planes in microphase-separated block copolymers, etc. Our interest is centered upon the phenomena of slip in entangled polymer−polymer interfaces. As such, slip in such situations is understood to occur as a result of the interspecies entanglements in the interfacial region and can arise even in situations wherein the incompatible polymers possess identical bulk rheological properties. In this section, we utilize the KN framework to propose a quantitative measure for the interspecies entanglements and thereby discern the explicit variations of the slip with the degree of incompatibility between the polymers.

DeGennes and co-workers have proposed a simple scaling argument to predict the slip arising during the shear of entangled polymer−polymer interfaces.[39,43] Their arguments (omitted here to maintain brevity) correlated the slip phenomena to the differences between the viscosity of an interfacial region and the bulk sample. They claimed that such differences arose primarily due to a lower probability to form an active entanglement in the interfacial region. This hypothesis led to an expression for the interfacial viscosity η_{in} as

$$\eta_{in} = f_e \eta_B \tag{9}$$

where η_B represents the scale-dependent bulk viscosity (i.e., the viscosity of a bulk sample with dimensions of the interface width) and f_e denotes the probability of forming an *interpenetrating entanglement* within the interface. DeGennes supplemented the above expression with a model relating f_e to the degree of incompatibility χ. Explicitly, by proposing that only interfacial chain strands of length greater than N_e can form entanglements, he derived the expression $f_e \sim \exp(-\chi N_e)$. In this work, we have adopted the approach of KN which replaces the picture of entanglements by an equivalent concept of constraints (as quantified by the coordination number $\bar{N}$). In such a framework, the above arguments can be viewed as an explicit relationship between the interfacial viscosity and the *number of interpenetrating constraints* between the incompatible polymer components. Indeed, a decrease in the number of constraints (resulting from increased incompatibility) leads to an increase in the mobility of the chain and in turn manifests as a decrease in the viscosity. In other words, if Ψ denotes the total number of interpenetrating constraints between the A and B polymers, then we interpret deGennes arguments as equivalent to $\Psi \sim \exp(-\chi N_e)$.

To facilitate an explicit comparison of our simulation results with the analytical arguments, we propose quantities termed as the "local degrees of interpenetration", denoted as $\psi_A(\mathbf{r})$ and $\psi_B(\mathbf{r})$, and defined as

$$\psi_A(\mathbf{r}) = \phi_A(\mathbf{r})\, \bar{N}_A^B(\mathbf{r}); \quad \psi_B(\mathbf{r}) = \phi_B(\mathbf{r})\, \bar{N}_B^A(\mathbf{r}) \tag{10}$$

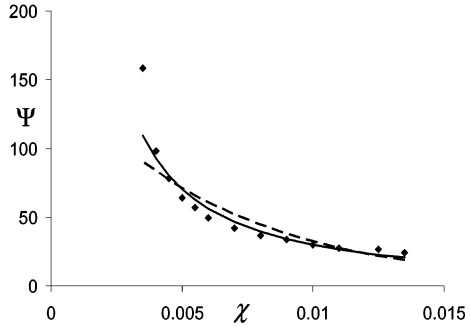

Figure 7. Dependence of the total number of interpenetrating constraints Ψ (in arbitrary units) upon the degree of incompatibility between the polymers. Also depicted are the best fit power law curve $\Psi = 0.1\chi^{-1.23}$ (solid line) and an exponential fit $\Psi = 157 \exp(-156.6\chi)$ (dotted line) to the numerical results.

In the above equation, $\bar{N}_A^B(\mathbf{r})$ denotes the total number of constraints which are imposed by the B chains on a A chain located at the position **r**. Analogously, $\bar{N}_B^A(\mathbf{r})$ denotes the total number of constraints imposed by the A chains on a B chain which is located at **r**. Note that in this notation we have $\bar{N}_A(\mathbf{r}) = \bar{N}_A^B + \bar{N}_A^A$. To address the role of incompatibility in a systematic manner, we consider the total number of interpenetrating constraints, Ψ, defined as

$$\Psi = \int d\mathbf{r}\, [\psi_A(\mathbf{r}) + \psi_B(\mathbf{r})] \tag{11}$$

We believe that this quantity (when appropriately normalized), which represents the total number of constraints between the incompatible species, possesses the closest relationship to the probability of an interspecies entanglement. Indeed, as one might expect, in the limit of complete miscibility Ψ behaves as an extensive quantity which scales with the volume of the sample, and hence the slip vanishes. In the opposite limit corresponding to ideal incompatibility, Ψ vanishes, and the situation corresponds to perfect slip. (It is to be noted however that the latter limit is preceded by a crossover from an entangled to a Rouse interface, wherein a different mechanism of slip manifests.) Having noted that the quantity Ψ exhibits appropriate behavior in the different limits, it is of interest to probe whether indeed this quantity varies in the manner suggested by the scaling arguments of deGennes. Figure 7 displays the variation of Ψ as a function of the degree of incompatibility χ. As might be expected, it is indeed observed that the total number of interpenetrating constraints decreases monotonically with an increase in the incompatibility between the polymers. This suggests that the relative friction between the chains decreases, and hence the slip between the polymers increases with an increase in the incompatibility. However, in contrast to the analytical arguments, the variation of this quantity is seen to be more consistent with a power law (as depicted in Figure 7) than the proposed exponential decay and consequently appears to be a much weaker function of the degree of incompatibility than predicted. We are not aware of any experiments that have systematically probed the effects of incompatibility upon the magnitude of the slip. The preceding result however constitutes an experimentally verifiable proposition, a confirmation of which would lend support to the KN picture of entanglements as well as the other results presented in this article.

B. Toughness of Polymer Interfaces. The adhesion characteristics and the failure mechanisms of polymer−polymer interfaces play an important role in a variety of applications. Over the past decade, considerable advances have been achieved in the pursuit of systematically delineating the features governing such characteristics. A number of careful experiments,[38,48,49] mainly led by Kramer, Creton, Brown, and co-workers (cf. ref 42 for a recent review), have elaborated the different failure mechanisms of polymer interfaces in terms of generalized phase diagrams correlating the fracture toughness (denoted G_C) to the areal density of entangled polymers at the interface (denoted as Σ). For instance, in situations involving low areal densities of polymers, interfaces are speculated to fail by a chain pullout mechanism, and the fracture toughness G_C is predicted to be proportional to Σ.[47] In contrast, at higher areal densities, other mechanisms such as those involving the crazing of the interface becomes the dominant mode of failure. In such a regime, and when the failure mechanism involves only a single wide crack-tip craze, experimental results as well as a theoretical model advanced by Brown[40] support the scaling $G_C \sim \Sigma^2$.

In a recent article, Brown[38] tried to develop an explicit functional form for a relationship between the fracture toughness G_C of different pairs of immiscible polymers and the width of the interface between them (denoted a_I) by employing three simplifying assumptions: (i) Entanglements can be viewed as stress supporting junctions. (ii) Entanglements are uniformly distributed throughout the chain: In other words, the entanglement length N_e is assumed to be a constant independent of the location of the chain. (ii) The total number of chain segments whose adjacent entanglements occur on the different sides of the interface constitutes a measure of the areal density of entanglements Σ. By utilizing these assumptions, Brown developed an analytical expression for Σ and demonstrated that the model agreed reasonably well with the experimental results in situations wherein the interfacial thickness was much larger than the length of an entanglement strand. Further, he speculated that a proper accounting for the changes in the entanglement length in the interfacial zone might improve the correspondence of the results for smaller interfacial thicknesses.

In the present section, we wish to probe whether indeed spatial inhomogeneities in the entanglement lengths (as predicted in this article) can validate the theory of Brown for the entire range of interfacial thicknesses. At the outset, we revisit the model and the arguments proposed by Brown.[38] The crux of Brown's analytical expressions was based on a prescription for a quantity $p(z,z')$ representing the probability that a strand of the chain which has an entanglement at the position z ($z < 0$) has the next entanglement (after N_e monomers) at the position z' ($z' > 0$). Explicitly, he postulated that

$$p(z,z') \propto \frac{\phi(z')}{\phi(z)} \tag{12}$$

where $\phi(z)$ and $\phi(z')$ denote the volume fractions of the species at the positions z and z', respectively. Further, he defined the areal density of the strands, Σ, in terms of this quantity $p(z,z')$ as

$$\Sigma \propto \int_0^{L_e} dz \int_0^{L_e - z} dz' \, \phi(z) \, p(z,z') \tag{13}$$

where L_e denotes the entanglement length as expressed in spatial dimensions. By utilizing the density profile $\phi(z)$ as calculated from self-consistent-field theory, Brown was able to relate the areal density of the strands Σ to the interfacial width. To effect an accurate validation of the model, we undertook simulations to compute the total probability that two arbitrary monomers s and $s + N_e$ along the chain are on the opposite sides of the interface. Explicitly, such simulations were performed by utilizing random walk statistics (cf. section IV for details of the simulation approach) to compute the number of A chains that start at the A side of the interface and whose end after N_e steps lies on the B side of the interface. Within the framework outlined by Brown, the areal density of the strands Σ is then related to this probability (denoted $\hat{p}$) by

$$\Sigma \propto \hat{p} \tag{14}$$

In Figure 8, we display the variations of the normalized toughness [defined as $\Sigma^2(\chi)/\Sigma^2(\chi=0)$] as a function of the nondimensionalized interface thickness. The results portrayed considers three different models: (i) the analytical expression proposed by Brown, (ii) numerical values of $\hat{p}$ computed employing a homogeneous entanglement length N_e, and (iii) numerical values of $\hat{p}$ computed employing an inhomogeneous entanglement length $N_e(z)$. To facilitate comparisons, the experimental results published by Brown[38] are also shown alongside these numerical values. Since the approach discussed in the preceding sections eschewed a computation of the inhomogeneities in the entanglement length, for the latter quantity we employed a simple prescription (which serves as an upper bound) proposing that the entanglement length and the coordination numbers are inversely related; in other words, $N_e(z) = N_e^H(\bar{N}^H/\bar{N}(z))$, where N_e^H and $\bar{N}^H$ denote the entanglement lengths and coordination numbers in a homogeneous melt. It is evident from the results displayed that the numerical values of the scaled toughness (computed employing both homogeneous and inhomogeneous entanglement lengths) prove quite inaccurate in accounting for the experimental results. In addition, it is also seen that the analytical expression proposed by Brown severely overpredicts the numerical values of the probabilities computed from our simulations. We believe that the prescription, viz., eq 12, proposed by Brown is not a very accurate description of the physics at hand (cf. refs 51 and 52 for a more sophisticated approach in the context of grafted interfaces). Indeed, eq 12 does not account for the fact that the monomers under consideration are separated along the contour of the chain by the entanglement length N_e. Consequently, we expect that his expressions would serve only as a upper bound to the desired quantity. These numerical results together suggest that the physically motivated quantity proposed by Brown, viz., the total number of chain segments with adjacent entanglements on the different sides of the interface, might not be completely adequate in embodying all the features requisite to correlating the toughness of the interfaces. In the following, we analyze the efficacy of an alternative measure in correlating the experimental results.

It is reasonable to expect that the fracture toughness would indeed correlate with some measure of the areal density of the interfacial entanglements. We propose empirically that the following quantity

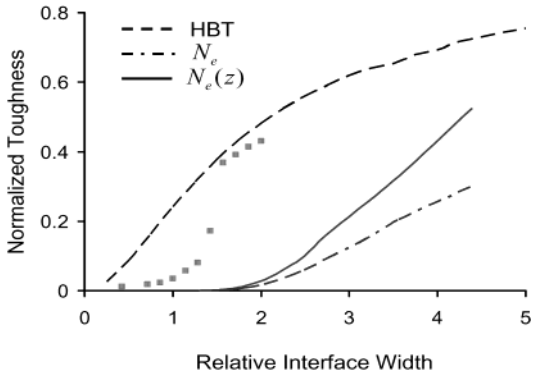

Figure 8. Dependence of the normalized toughness of the interface on the relative interface width. The latter represents a nondimensional measure of the interface width and is defined as a_I/L_e. In the above figure, HBT represents the results calculated using the analytical expression proposed by Brown. The curves labeled N_e and $N_e(z)$ respectively represent the results of our Monte Carlo simulations assuming constant and inhomogeneous entanglement lengths. The unconnected points represent the experimental results presented in Brown.[38]

$$\Omega = \int_{-L_e}^{L_e} dz \, [\psi_A(z) + \psi_B(z)] \tag{15}$$

embodies the closest physical connection to such a concept and might serve to quantify the areal density of interfacial entanglements in a more effective manner.[51,52] In essence, this quantity provides a measure of the total number of interpenetrations within a distance L_e from the dividing surface of the interface. By postulating further that the interpenetrating entanglements in this region are more likely to have their next entanglements in the respective phases, it is evident that Ω possesses a physical meaning similar to the quantity defined by Brown. Consequently, we expect $\Omega \propto \Sigma$ or, in other words, $G_C \propto \Omega^2$. However, it is to be noted that in the interfacial region the coordination numbers and the entanglement lengths exhibit inhomogeneous variations, that is, $N_e \equiv N_e(z)$ and $L_e \equiv L_e(z)$. Nevertheless, consistent with the degree of empiricism already embodied in the definition of eq 15, in the following we treat L_e as a spatially constant quantity corresponding to its value in a homogeneous melt.

Figure 9 depicts the variation of the normalized toughness (now defined as $\Omega^2(\chi)/\Omega^2(\chi = 0)$] as a function of the nondimensionalized interfacial thicknesses which were determined from our simulations. It is important to note that our simulations were effected with a finite chain length corresponding to $N = 1000$. It is however well documented that the interfacial thickness does depend significantly on the precise value of the chain length.[48,50] In contrast, the quantity Ω quantifies the degree of interpenetrations within the interfacial region and is expected to be only a weak function of the chain length N. Consequently, to eliminate the spurious dependencies arising from the finiteness of the chain length, we have also displayed the numerical results for Ω explicitly as a function of the interfacial thickness corresponding to $N = \infty$. [This quantity was taken to be identical to the Helfand−Tagami prediction,[37] $a_I(N=\infty) = 2b/(6\chi)^{1/2}$.] It is evident from the results that the numerical values of this rescaled Ω correlates the experimental observations much closer than any of the other theoretical approaches we analyzed. One cannot

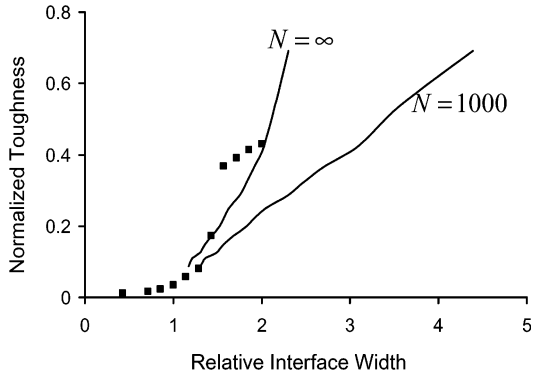

Figure 9. Dependence of the normalized interfacial toughness (defined based on the interpenetrating entanglements) on the relative interfacial width. Shown explicitly are the results from our numerical simulation ($N = 1000$ and $N = \infty$), wherein the interfacial width was determined using the numerical density profiles. The interface thicknesses for the latter situation are obtained using the Helfand−Tagami formula.[37] The numerical results correspond to a $L_e = 3$ (in units of Kuhn segment length), and the experimental results correspond to a $L_e \sim 7$ nm.

however expect the steep variation displayed by the numerical curves to persist for large interfacial widths (by construction of a *normalized* measure we have assured its saturation), and consequently we expect that the shape of the curve to change for larger interfacial widths. While we can speculate that these changes might start resembling the sigmoidal curves measured in experiments, our current numerical capabilities (requiring significantly large simulation cells) do not allow for a straightforward probe of such regimes. By a power law extrapolation fit to the curve displayed, we can estimate that the scaled toughness saturates at its maximum value at an interfacial thickness of around $2.5L_e$, which is consistent with the experimental observations which noticed a saturation of the toughness beyond about $1.5L_e$.[38,48,49] The preceding results are very suggestive of the claim that the degree of interpenetrating entanglements can indeed serve as an effective measure to correlate the fracture toughness of the interface.

Our primary motivation in this section was to analyze the impact of inhomogeneities in entanglement lengths in accounting for the inadequacies of Brown's original model. However, in such an effort we demonstrated that neither the original approach nor that incorporating inhomogeneous entanglements can account for the experimental results. As an alternative, we have taken recourse to the concept of entanglement interpenetrations proposed in the preceding section. Our numerical results indicate that a new measure Ω quantifying the total number of entanglement interpenetrations in a region of width corresponding to the entanglement length might serve to correlate the experimental results in a more accurate manner. However, while our numerical results seem to fall in the range of experimental measurements, several features are still not captured. For instance, the experimental results exhibit a characteristic sigmoidal shape which is not reflected in the numerical results presented. Furthermore, the numerical results also need to be corrected to probe for parameters identical to the experimental measurements. Needless to emphasize, further systematic experiments and comparisons are necessary to validate our proposal.

Summary. In summary, in this section we have tried to establish some connections between the approach and the results of this research to the rheological and mechanical properties of polymer interfaces. Our efforts centered upon the concept of "interpenetrating entanglements" which hitherto was a unexplored idea. By utilizing this concept, we put forth a number of physically motivated proposals relating to the mechanical properties of polymer interfaces. Where possible, we have tried to establish connections to existing experimental results. However, as we have emphasized at the outset, many of the ideas proposed in this section are empirical and were motivated by an objective to derive "experimentally verifiable" consequences of the theory proposed in this article. Consequently, we hope that this section would motivate future experiments and experimentalists to analyze and validate the ideas proposed.

VIII. Summary and Outlook

In summary, this article presented a systematic analysis of the interplay between the compositional inhomogeneities, chain conformations, and the entanglement lengths in multicomponent polymeric mesophases. To effect this objective, we modified the packing approach proposed by Kavassalis and Noolandi to account for the presence of compositional inhomogeneities. Our research was primarily directed toward the clarification of fundamental issues pertaining to interfacial entanglements in polymer blends. Explicitly, we demonstrated that the compositional inhomogeneity and the accompanying changes in the chain conformations can lead to significant changes in the entanglement lengths, by even up to a factor of 2 in strongly incompatible mixtures. While such changes clarified the interplay between the inhomogeneity and entanglements at a microscopic level, we also undertook to relate the approach and the results presented in this article to experimentally verifiable macroscopic consequences, especially relating to the mechanical properties of polymer interfaces. In the pursuit of such an objective, we proposed a new concept "interpenetrating entanglements", which we related to the slip and toughness of polymer interfaces. While we tried to establish connections to existing theoretical and experimental literature, we believe that further systematic experiments are necessary to validate the many new and empirical proposals elaborated in this article.

The present research lends itself to many developments which we hope to pursue in future publications. At a computational level, our approach can be embellished and rendered more accurate by replacing the lattice model and cubic elements by continuum approaches employing noncubic elements. In addition, in the regimes of strong stretching and/or in systems involving non-Gaussian polymers, the chains are expected to exhibit significant orientational effects arising as a consequence of the compositional inhomogeneity and can therefore constitute model systems for the reexamination of the utility of a single isotropic value for the coordination number to describe entanglements. It is also to be noted that recently Theodorou and coworkers[51,52] have developed a novel simulation approach to generate an entanglement network for grafted polymer−polymer interfaces and have employed it to probe the density of interpenetrating entanglements at an interface. We hope to utilize such an approach to provide a link between the KN viewpoint analyzed in this article

with the alternative junction viewpoint of entanglements. At a more fundamental level, one can employ the approach presented in this article toward a clarification of entanglements in situations involving polymer−solid films. In fact, a number of researchers have demonstrated profound influences on the dynamics of the entangled polymer chains in confined environments.[53] Inhomogeneous entanglements and its role in influencing such effects have not been addressed in the literature. Another line of research would involve translating the ideas presented herein to a model for the dynamics of entangled inhomogeneous phases. Indeed, as we had repeatedly stressed in the Introduction, it is not obvious whether the inhomogeneous entanglement length we have computed would play the same role in the dynamics as that played by the entanglement length of a homogeneous melt. Development of appropriate microscopic dynamical models and/or simulation tools can serve to clarify this issue.[41] We also hope that the present work will stimulate more experiments designed to probe the macroscopic consequences we have outlined. A successful validation by such methods would lend support to a different viewpoint of entanglements which might prove more relevant for inhomogeneous situations.

Note in Proof. After we completed this paper, we became aware that Prof. Hugh Brown was preparing a manuscript on similar issues, albeit by adopting a somewhat different approach. A comparison of our results with the preliminary results sent to us by Prof. Brown indicated a good agreement on the main qualitative features. We are grateful to Prof. Brown for many significant insights and his comments pertaining to this work.

Acknowledgment. This work was partially supported by National Science Foundation under Award DMR-02-04199. Acknowledgment is also made to the donors of the Petroleum Research Fund, administered by the ACS, for partial support of this research. We thank Mr. Jason Benkwoski and Profs. Glenn Fredrickson, Ron Larson, Ken Schweizer, and Ed Kramer for stimulating discussions and encouragement on this research.

References and Notes

(1) Green, M.; Toblosky, A. *J. Chem. Phys.* **1946**, *14*, 80. Lodge, A. *Trans. Faraday Soc.* **1956**, *52*, 120. Yamamoto, M. *J. Phys. Soc. Jpn.* **1956**, *11*, 413.
(2) deGennes, P. G. *J. Chem. Phys.* **1971**, *55*, 572.
(3) Doi, M.; Edwards, S. F. *J. Chem. Soc., Faraday Trans.* **1978**, *74*, 1789; *J. Chem. Soc., Faraday Trans.* **1978**, *74*, 1802; *J. Chem. Soc., Faraday Trans.* **1978**, *74*, 1818.
(4) Watanabe, H. *Prog. Polym. Sci.* **1999**, *24*, 1253.
(5) Lin, Y. H. *Macromolecules* **1987**, *20*, 3080.
(6) Kavassalis, T. A.; Noolandi, J. *Phys. Rev. Lett.* **1987**, *59*, 2674.
(7) Kavassalis, T. A.; Noolandi, J. *Macromolecules* **1989**, *22*, 2709.
(8) Kavassalis, T. A.; Noolandi, J. *Macromolecules* **1988**, *21*, 2869.
(9) Wu, S. *J. Polym. Sci., Part B: Polym. Phys.* **1989**, *27*, 723.
(10) Ronca, G. *J. Chem. Phys.* **1993**, *79*, 1031.
(11) Fetters, L. J.; Lohse, D. J.; Richter, D.; Witten, T. A.; Zirkel, A. *Macromolecules* **1994**, *27*, 4639.
(12) Heymans, N. *Macromolecules* **2000**, *33*, 4226.
(13) Fetters, L. J.; Lohse, D. J.; Milner, S. T.; Graessley, W. W. *Macromolecules* **1999**, *32*, 6847.
(14) Fetters, L. J.; Lohse, D. J.; Graessley, W. W. *J. Polym. Sci., Part B: Polym. Phys.* **1999**, *37*, 1023.
(15) Wool, R. P. *Macromolecules* **1993**, *26*, 1564.
(16) Hamley, I. W. *Block Copolymers*; Oxford University Press: Oxford, 1999.
(17) Bates, F. S.; Fredrickson, G. H. *Phys. Today* **1999**, *52* (2), 32.
(18) Brown, H. R.; Russell, T. P. *Macromolecules* **1996**, *29*, 798.
(19) Bitsannis, I. A.; ten Brinke, G. *J. Chem. Phys.* **1993**, *99*, 3100.
(20) Wang, J. S.; Binder, K. *J. Phys. I* **1991**, *1*, 1583.
(21) Kumar, S. K.; Vacatello, M.; Yoon, D. Y. *Macromolecules* **1990**, *23*, 2189.
(22) Fischel, L. B.; Theodorou, D. N. *J. Chem. Soc., Faraday Trans.* **1995**, *91*, 2382.
(23) Almdal, K.; Rosedale, J. H.; Bates, F. S.; Wignall, G. D.; Fredrickson, G. H. *Phys. Rev. Lett.* **1990**, *65*, 1112.
(24) Murat, M.; Grest, G. S.; Kremer, K. *Europhys. Lett.* **1998**, *42*, 401.
(25) Pan, X.; Schaffer, J. S. *Macromolecules* **1996**, *29*, 4453.
(26) Richter, D.; Farago, B.; Butera, R.; Fetters, L. J.; Huang, J. S.; Ewen, B. *Macromolecules* **1993**, *26*, 795.
(27) Semenov, A. N. *Phys. Rev. Lett.* **1998**, *80*, 1908. Fredrickson, G. H. *J. Chem. Phys.*, in press.
(28) Schmid, F. *J. Phys.: Condens. Matter* **1998**, *10*, 8105.
(29) Fredrickson, G. H.; Ganesan, V.; Drolet, F. *Macromolecules* **2002**, *35*, 16.
(30) Matsen, M. W. *J. Phys.: Condens. Matter* **2002**, *14*, 21.
(31) Edwards, S. F. *Proc. Phys. Soc. London* **1965**, *85*, 613.
(32) Helfand, E. *J. Chem. Phys.* **1975**, *62*, 999.
(33) Matsen, M. W.; Schick, M. *Phys. Rev. Lett.* **1994**, *72*, 2660.
(34) Drolet, F.; Fredrickson, G. H. *Phys. Rev. Lett.* **1999**, *83*, 4317.
(35) Chen, H.-Y.; Fredrickson, G. H. *J. Chem. Phys.* **2002**, *116*, 1137.
(36) Thompson, R. B.; Ginzburg, V. V.; Matsen, M. W.; Balazs, A. C. *Science* **2001**, *292*, 2469.
(37) Helfand, E.; Tagami, Y. *J. Chem. Phys.* **1971**, *56*, 3592.
(38) Brown, H. R. *Macromolecules* **2001**, *34*, 3720.
(39) deGennes, P. G. *C. R. Acad. Sci. (Paris), Ser. II* **1989**, *308*, 1401.
(40) Brown, H. R. *Macromolecules* **1991**, *24*, 2752.
(41) Goveas, J. L.; Fredrickson, G. H. *Eur. Phys. J. B* **1998**, *2*, 79.
(42) Creton, C.; Kramer, E. J.; Brown, H. R.; Hui, C. Y. *Adv. Polym. Sci.* **2002**, *156*, 53.
(43) Brochard-Wyart, F.; deGennes, P. G. *C. R. Acad. Sci. (Paris), Ser. II* **1990**, *310*, 1169.
(44) Ajdari, A. *C. R. Acad. Sci. (Paris), Ser. II* **1993**, *317*, 1159.
(45) Zhao, R.; Macoscko, C. W. *J. Rheol.* **2002**, *46*, 145.
(46) Doi, M.; Harden, J. L.; Ohta, T. *Macromolecules* **1993**, *26*, 4935.
(47) Washiyama, J.; Kramer, E. J.; Hui, C. Y. *Macromolecules* **1993**, *26*, 2928.
(48) Schnell, R.; Stamm, M.; Creton, C. *Macromolecules* **1998**, *31*, 2284.
(49) Schnell, R.; Stamm, M.; Creton, C. *Macromolecules* **1999**, *32*, 3240.
(50) Broseta, D.; Fredrickson, G. H.; Helfand, E.; Leibler, L. *Macromolecules* **1990**, *23*, 132.
(51) Terzis, A. F.; Theodorou, D. N.; Stroeks, A. *Macromolecules* **2000**, *33*, 1385.
(52) Terzis, A. F.; Theodorou, D. N.; Stroeks, A. *Macromolecules* **2000**, *33*, 1397.
(53) Jones, R. A. L. *Curr. Opin. Colloid Interface Sci.* **1999**, *4*, 153.

MA020930Y